



Short communication

Carbon nanofiber supported bimetallic PdAu nanoparticles for formic acid electrooxidation

Yuan-Hang Qin^{a,b}, Yue Jiang^a, Dong-Fang Niu^a, Xin-Sheng Zhang^{a,*}, Xing-Gui Zhou^a, Li Niu^c, Wei-Kang Yuan^a

^aState Key Laboratory of Chemical Engineering, East China University of Science and Technology, Shanghai 200237, China

^bKey Laboratory for Green Chemical Process of Ministry of Education, Wuhan Institute of Technology, Wuhan 430074, China

^cState Key Laboratory of Electroanalytical Chemistry, Chang Chun Institute of Applied Chemistry, Chinese Academy of Sciences, Changchun 130022, China

HIGHLIGHTS

- CNF supported high-alloying PdAu nanoparticles are successfully synthesized.
- The high-alloying PdAu/CNF exhibits a good activity for formic acid electrooxidation.
- The electronic effect of Au on Pd for formic acid oxidation is proposed.

ARTICLE INFO

Article history:

Received 5 April 2012

Received in revised form

4 May 2012

Accepted 5 May 2012

Available online 12 May 2012

Keywords:

Carbon nanofiber

Formic acid oxidation

Alloy

Formic acid fuel cells

ABSTRACT

Carbon nanofiber (CNF) supported PdAu nanoparticles are synthesized with sodium citrate as the stabilizing agent and sodium borohydride as the reducing agent. High resolution transmission electron microscopy (HRTEM) characterization indicates that the synthesized PdAu particles are well dispersed on the CNF surface and X-ray diffraction (XRD) characterization indicates that the alloying degree of the synthesized PdAu nanoparticles can be improved by adding tetrahydrofuran to the synthesis solution. The results of electrochemical characterization indicate that the addition of Au can promote the electrocatalytic activity of Pd/C catalyst for formic acid oxidation and the CNF supported high-alloying PdAu catalyst possesses better electrocatalytic activity and stability for formic acid oxidation than either the CNF supported low-alloying PdAu catalyst or the CNF supported Pd catalyst.

© 2012 Elsevier B.V. All rights reserved.

1. Introduction

The electrooxidation of formic acid has attracted increasing attention due to the promising application of direct formic acid fuel cells (DFAFCs) [1–3]. It is now generally recognized that the formic acid electrooxidation proceeds through a dual-path mechanism whereby one path is the direct oxidation of formic acid via dehydrogenation and the other is the oxidation of formic acid via an adsorbed CO intermediate that is formed by dehydration of formic acid [4,5]. The previous studies have revealed that Pd in nanoparticle forms can catalyze the oxidation of formic acid at the anode of DFAFCs with greater resistance to CO than Pt catalysts [4,6].

Although Pd shows higher electrocatalytic activity for formic acid oxidation than Pt, the activity and stability of Pd catalyst are still in need of improvements to meet the requirements of the anode catalyst in DFAFCs and much effort has therefore been devoted to synthesize and develop novel Pd-based catalysts. It is reported that the catalytic activity and stability of Pd catalyst for formic acid oxidation could be improved by the addition of metal or metal oxide promoters [6–8]. Among the Pd-based catalysts, Pd–Au binary system has attracted the most attention. Masel et al. [6] discovered that the addition of Au to the carbon supported Pd catalyst could aid the electrooxidation of formic acid in some manner through either electronic modification of the catalyst, a two-body effect or catalytic activity of Au toward poisons/formic acid. However, the PdAu particle size in the PdAu/C catalyst synthesized by Masel et al. is very large and the size distribution is quite broad [6]. It is well known that small particle size could offer more active sites for carrying catalytic reactions. Therefore,

* Corresponding author. Tel.: +8621 64253469; fax: +8621 64253528.

E-mail address: xszhang@ecust.edu.cn (X.-S. Zhang).

synthesis of PdAu nanoparticles with relatively small particle size and narrow size distribution appears to be significantly desirable.

In addition to the particle size, the catalytic properties of Pd–Au catalysts are highly dependent on their structure (e.g., core–shell structure, alloy) [9]. Zhou et al. [10] prepared the carbon supported bimetallic Au–Pd nanoparticles with a core–shell structure and found that the core–shell structure of bimetallic Au–Pd catalyst not only enhanced the Pd activity in formic acid electro-oxidation but also improved the catalyst stability due to the interaction between Pd shell and Au core. Hsing et al. [9] prepared alloy and non-alloy bimetallic PdAu nanoparticles using a right rate-limiting strategy and found that the PdAu alloys exhibited higher Pd-specific activities toward formic acid oxidation compared with the non-alloy counterpart or individual Pd catalyst. Hence the synthesis of high-alloying PdAu nanoparticles with small particle size for formic acid oxidation appears to be highly desirable.

The synthesis of Au and Pd nanocrystals by citrate reduction could be used as a guide in the preparation of PdAu particles with small particle size and narrow size distribution [11–14]. Turkevich reported the synthesis of Au and Pd nanocrystals with a relatively narrow size distribution by citrate reduction method, which involves the reaction of hot Au and Pd precursors with trisodium citrate solution [11,12]. In the Turkevich method, Au and Pd nanocrystals with controllable particle size could be synthesized because the citrate ions act as both reducing and stabilizing agents. It is reported that the residual citrate could be easily removed by washing with deionized water [15], which is another merit of the Turkevich method because a clean, stabilizing agent-free particle surface is highly desirable to maintain catalytic activities of the as-synthesized nanoparticles.

The synthesis of high-alloying PtRu nanoparticles by a chemical reduction method in a tetrahydrofuran–water (THF–H₂O) solution could be used as a guide in the preparation of high-alloying PdAu nanoparticles [16,17]. In this work, highly alloyed and highly dispersed PdAu nanoparticles were supported on carbon nanofibers (CNFs) by a modified Turkevich method with trisodium citrate as stabilizing agent and NaBH₄ as reducing agent in a THF–H₂O solution, and the catalytic activity of the high-alloying PdAu/CNF catalyst for formic acid oxidation was compared with those of the low-alloying PdAu/CNF catalyst and the Pd/CNF catalyst.

2. Experimental

The CNFs used here were platelet type CNFs, which were synthesized and purified according to the literature [18]. Sonochemical oxidation treatment was employed to import oxygen-containing functional groups onto CNFs [19,20]. The following section describes the detailed synthesis procedure of the high-alloying PdAu/CNF catalyst with a mass ratio of Pd:Au = 3:1. First, 1.762 mL of 0.1 M PdCl₂·2H₂O (in 0.1 M HCl) and 653.4 μL of 0.04856 M AuCl₃·HCl·4H₂O were added dropwise to a stirred 10 mL of 20.8 mM trisodium citrate solution which was kept at 10 °C and subsequently the pH value of the solution was adjusted to 5.5 by adding 0.02 M NaOH solution. Then the above solution was added dropwise to a stirred 20 mL (10 mL THF+10 mL water) of 5 mg mL⁻¹ CNF slurry. After 18 h of stirring at 10 °C, 15 mL of 0.3 M freshly prepared ice-cold NaBH₄ solution was added to the above solution in a dropwise manner. The solution was stirred for additional 3 h at 10 °C. The resulted material was filtered and washed with deionized water and then dried at 80 °C overnight. The high-alloying PdAu/CNF catalyst with a total noble metal loading of 20 wt. % was obtained. And Au/CNF catalyst with an Au loading of 20 wt. % was prepared by the same procedure. For comparison,

a low-alloying PdAu/CNF catalyst and a Pd/CNF catalyst each with a total noble metal loading of 20 wt. % were prepared with the same procedure except that water was used instead of THF/water for CNF slurry preparation. The low- and high-alloying PdAu/CNF catalysts were denoted as Pd₃Au₁/CNF-I and Pd₃Au₁/CNF-II, respectively. The noble metal loadings of the catalysts determined by inductively coupled plasma atomic emission spectroscopy (ICP-AES, Thermo Elemental IRIS 1000) analyses were consistent with the nominal values.

X-ray diffraction (XRD) patterns of the obtained catalysts were recorded on an X-ray diffractometer (D/MAX 2550 VB/PC, RIGAKU) using Cu Kα as radiation source ($\lambda = 0.154056$ nm). High resolution transmission electron microscopy (HRTEM FEI Tecnai G2 F30 S-Twin) was used for particle size and size distribution analyses. Electrochemical characterization was performed on a PGSTAT 30 electrochemical workstation (Eco Chemie B.V., The Netherlands). All experiments were conducted in a three-electrode system at 18 ± 1 °C. The working electrode was prepared as follows. A suspension of Pd₃Au₁/CNF (Pd/CNF) ink was prepared by ultrasonically dispersing 1 mg of Pd₃Au₁/CNF (Pd/CNF or Au/CNF) in 90 μL of ethanol and 10 μL of Nafion (5 wt. %) solution for 30 min. A 2 μL of the above solution was pipetted onto a glassy carbon (GC) electrode with 3 mm diameter, followed by solvent evaporation at room temperature. The loading of PdAu (Pd or Au) on the working electrode was 4 μg. A Pt foil and a saturated calomel electrode (SCE) were used as counter electrode and reference electrode, respectively.

3. Results and discussion

Fig. 1 shows the XRD patterns of Au/CNF, Pd/CNF, Pd₃Au₁/CNF-I and Pd₃Au₁/CNF-II catalysts. Positions of the diffraction peaks of Pd/CNF and Au/CNF catalysts fit well with their characteristic face centered cubic (fcc) patterns. It can be seen that the PdAu particles in the Pd₃Au₁/CNF-I catalyst exhibit two phases, a Pd-rich phase and an Au-rich phase, with the former being dominant because the Pd loading is much larger than the Au loading in the catalyst. While the PdAu particles in the Pd₃Au₁/CNF-II catalyst exhibit only a single phase with the diffraction peak positions located between those of pure Pd/C and Au/C, indicating that Pd and Au are highly alloyed, forming high-alloying PdAu particles. The crystallite sizes and lattice parameters of Pd/CNF, Pd₃Au₁/CNF-I and Pd₃Au₁/CNF-II

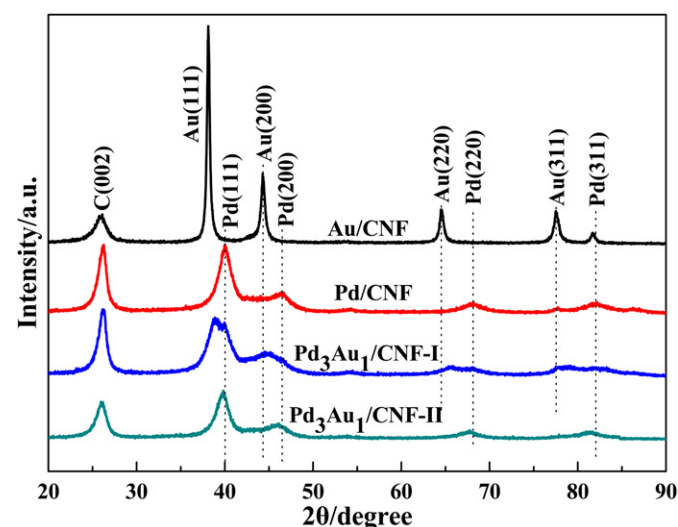


Fig. 1. XRD patterns of Au/CNF, Pd/CNF, Pd₃Au₁/CNF-I and Pd₃Au₁/CNF-II catalysts.

Table 1
XRD data of Pd/CNF, Pd₃Au₁/CNF-I and Pd₃Au₁/CNF-II catalysts.

Catalysts	Pd (111) at 20°	Crystallite size/nm	Lattice parameter/ nm	x _{Au} /%
Pd/CNF	40.04	4.0	0.3897	0
Pd ₃ Au ₁ /CNF-I	39.90	3.9	0.3910	7.1
Pd ₃ Au ₁ /CNF-II	39.78	5.5	0.3922	13.7

catalysts, calculated based on the diffraction peaks of Pd (111), are listed in **Table 1**.

As can be seen from **Table 1**, the 2θ values of Pd(111) of Pd₃Au₁/CNF-I and Pd₃Au₁/CNF-II are smaller than that of Pd/CNF, indicating that Au has entered into the Pd lattice forming PdAu alloy, as also evidenced by the lattice expansion due to the bigger radius of Au atom as compared with that of Pd atom. The 2θ value of Pd(111) of Pd₃Au₁/CNF-II was smaller than that of Pd₃Au₁/CNF-I, indicating that more Pd atoms in the Pd₃Au₁/CNF-II catalyst have been replaced by Au atoms and the alloying degree of PdAu in the Pd₃Au₁/CNF-II catalyst is higher than that in Pd₃Au₁/CNF-I catalyst. Based on the lattice parameters, the alloying degree could be estimated by Vegard's law [21], and the atomic fractions of alloying Au (x_{Au}) in the Pd₃Au₁/CNF-I and Pd₃Au₁/CNF-II catalysts are listed in **Table 1**. The atomic fraction of alloying Au (x_{Au}) in the Pd₃Au₁/CNF-II catalyst is close to the nominal atomic fraction of Au (x_{Au})

(15.3% based on the mass ratio Pd/Au=3:1), confirming the formation of high-alloying PdAu particles. While the atomic fraction of alloying Au (x_{Au}) in the dominant Pd-rich phase of Pd₃Au₁/CNF-I catalyst is less than half of the nominal atomic fraction of Au (x_{Au}), indicating the formation of low-alloying PdAu particles.

The different alloying degrees of PdAu nanoparticles in the Pd₃Au₁/CNF-I and Pd₃Au₁/CNF-II catalysts can be attributed to the effect of THF. Lu et al. [16] prepared Pt-Ru/C catalyst by a chemical reduction method in an aqueous solution and found that the alloying degree of PtRu particles could be improved by adding THF to the aqueous solution, which was believed to be due to the formation of the complex of THF and Pt precursor (H₂PtCl₆), leading to the simultaneous reduction of Pt and Ru and the easy formation of PtRu alloy. Lu et al. [17] also found that the addition of THF could improve the alloying degree of PdAu particles.

Fig. 2 shows the HRTEM images and the corresponding size distribution histograms of Au/CNF, Pd/CNF, Pd₃Au₁/CNF-I and Pd₃Au₁/CNF-II catalysts. It can be seen that the as-synthesized Pd(Au) particles are well dispersed in the four catalysts, indicating that the modified Turkevich method is powerful to synthesize particles with high and uniform dispersion. It is interesting to note that the PdAu nanoparticles in the Pd₃Au₁/CNF-I catalyst (**Fig. 2(c)**) have relatively small particle size and appear to be more uniform as compared with the pure Pd nanoparticles in the Pd/CNF catalyst (**Fig. 2(b)**). Similar phenomena were also observed by Lu

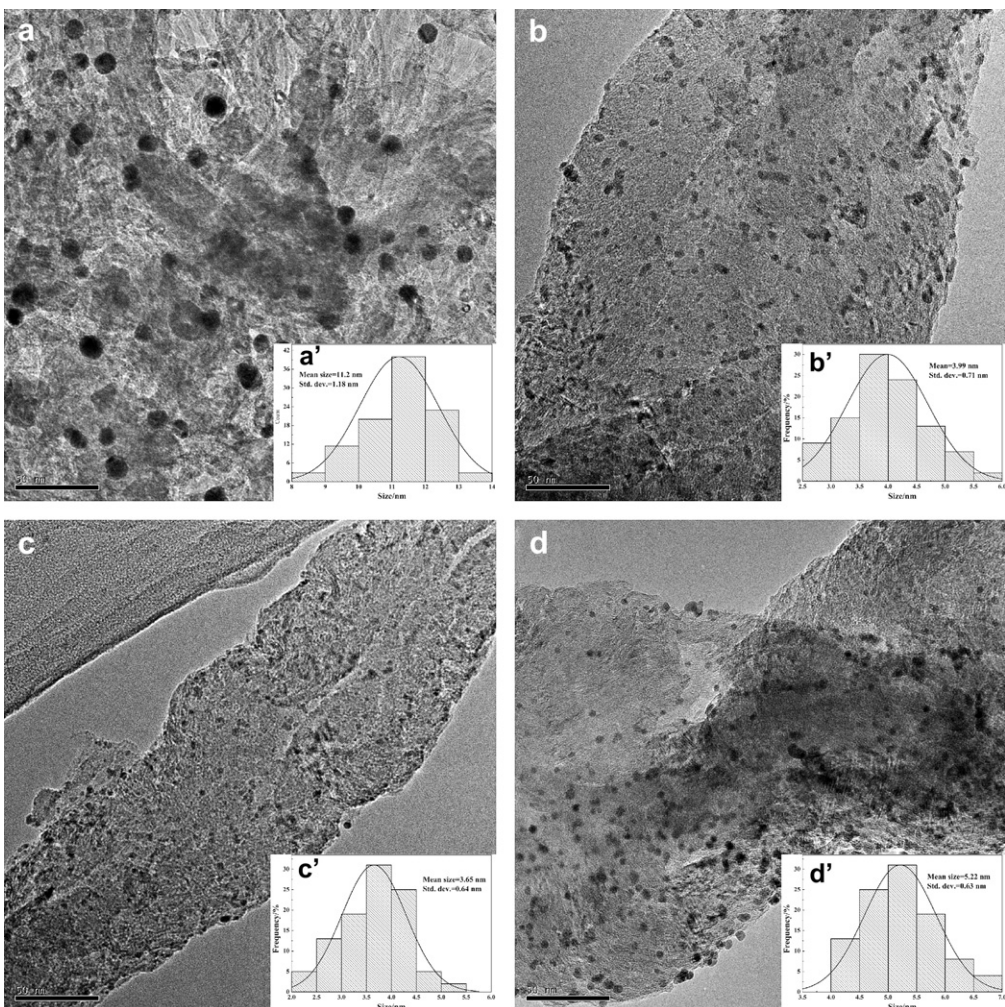


Fig. 2. HRTEM images and the corresponding particle size distribution histograms of Au/CNF (a), Pd/CNF (b), Pd₃Au₁/CNF-I (c) and Pd₃Au₁/CNF-II (d) catalysts.

et al. [22] in their synthesized PdIr nanoparticles and Masel et al. [6] in their synthesized PdAu nanoparticles, indicating that the addition of a second metal may have grain-refining effect. However, the mean particle size of $\text{Pd}_3\text{Au}_1/\text{CNF-II}$ catalyst is larger than those of Pd/CNF and $\text{Pd}_3\text{Au}_1/\text{CNF-I}$ catalysts, which may result from the reduced nucleation rate of PdAu particles in the presence of THF.

Fig. 3(a) shows the cyclic voltammograms of Pd/CNF, $\text{Pd}_3\text{Au}_1/\text{CNF-I}$ and $\text{Pd}_3\text{Au}_1/\text{CNF-II}$ catalysts in deaerated 0.5 M H_2SO_4 . All catalysts exhibit the typical hydrogen desorption/adsorption peaks ($-0.2\text{--}0$ V) and surface oxidation/reduction peaks (higher than 0.3 V). It is worth noting that the reduction peaks of surface oxide exhibit an anodic shift on $\text{Pd}_3\text{Au}_1/\text{CNF}$ catalysts compared with that on Pd/CNF catalyst. $\text{Pd}_3\text{Au}_1/\text{CNF-II}$ catalyst, in particular, exhibits the highest shift, indicating an easier removal of adsorbed oxygen species from high-alloying $\text{Pd}_3\text{Au}_1/\text{CNF-II}$ catalyst compared with that from low-alloying counterpart or Pd/CNF [9], which may result from the size and electronic effects. On larger Pd particles, easier removal of adsorbed oxygen species was observed [15]. The electronic effect in the high-alloying $\text{Pd}_3\text{Au}_1/\text{CNF-II}$ catalyst may also play a role in promoting the removal of adsorbed oxygen species, which will be discussed later.

Fig. 3(b) shows the cyclic voltammograms of Pd/CNF, Au/CNF, $\text{Pd}_3\text{Au}_1/\text{CNF-I}$ and $\text{Pd}_3\text{Au}_1/\text{CNF-II}$ catalysts in deaerated 0.5 M

$\text{H}_2\text{SO}_4+0.5$ M HCOOH. It can be seen that no oxidation peaks present for the Au/CNF catalyst, indicating that Au/CNF catalyst has no electrocatalytic activity for formic acid oxidation. The values of peak potential E_p and peak current density j_p of formic acid oxidation on Pd/CNF, $\text{Pd}_3\text{Au}_1/\text{CNF-I}$ and $\text{Pd}_3\text{Au}_1/\text{CNF-II}$ catalysts are listed in Table 2. As can be seen from the values of E_p and j_p that the $\text{Pd}_3\text{Au}_1/\text{CNF-II}$ catalyst exhibits the smallest E_p and the highest j_p values for formic acid oxidation, while the $\text{Pd}_3\text{Au}_1/\text{CNF-I}$ catalyst exhibits the highest E_p and the smallest j_p values, indicating that the alloying degree of PdAu particles has a significant effect on their electrocatalytic activity for formic acid oxidation.

The $\text{Pd}_3\text{Au}_1/\text{CNF-I}$ catalyst consists of two phases, a Pd-rich and an Au-rich phase, while the latter may have little or no electrocatalytic activity for formic acid oxidation, leading to low utilization of noble metals and low electrocatalytic activity of $\text{Pd}_3\text{Au}_1/\text{CNF-I}$ catalyst. It is worth noting that although Au-rich phase may have little or no electrocatalytic activity for formic acid oxidation, it may play a role in promoting Pd catalyst for formic acid oxidation. As can be seen from Table 2, the current density of formic acid oxidation on Pd/CNF catalyst (33.4 mA cm^{-2}) is 1.14 times larger than that on $\text{Pd}_3\text{Au}_1/\text{CNF-I}$ catalyst (29.2 mA cm^{-2}), while the Pd loading in the former is 1.25 times larger than that in the latter. In addition, a portion of Pd catalyst in the $\text{Pd}_3\text{Au}_1/\text{CNF-I}$ catalyst could not catalyze formic acid oxidation due to the possible coverage of Pd surface by Au-rich phase. Hence, the mass activity j_m (mA mgPd^{-1}) of $\text{Pd}_3\text{Au}_1/\text{CNF-I}$ catalyst will higher than that of Pd/CNF catalyst based on the Pd loading in the catalysts, as shown in Table 2.

Although the particle size of PdAu in $\text{Pd}_3\text{Au}_1/\text{CNF-II}$ catalyst is larger than that of Pd in Pd/CNF catalyst, the former exhibits a higher peak current density for formic acid oxidation than the latter, and one possible mechanism accounting for the increased activity is as follows. Based on Hammer's theory [23], the reactivity of metal catalyst is dependent on the position of d-band center. Based on theory calculations, Nørskov et al. [24] found that d-band in PdAu alloy shifted relative to Pd and Au. Lee et al. [10] found that Pd could obtain d-band electrons from Au in the Au@Pd/C (Au core Pd shell) catalyst, and this electronic effect reduced the adsorption strength of $-\text{COOH}_{\text{ads}}$ like intermediate species generated during formic acid oxidation on Pd surface, contributing to the release of surface active sites of Pd [9,10]. It is worth noting that the peak potential for formic acid oxidation increases in the order of $\text{Pd}_3\text{Au}_1/\text{CNF-II} < \text{Pd}/\text{CNF} < \text{Pd}_3\text{Au}_1/\text{CNF-I}$, which may mainly result from the particle size effect. Generally, Pd(110) and Pd(111) are more active than Pd(100), but Pd(110) surface in nanoparticles is not stable due to higher surface energy. An increase in Pd particle size leads to the increase of Pd(111) planes, thus larger Pd particles with more Pd(111) planes would be more active for formic acid oxidation [15].

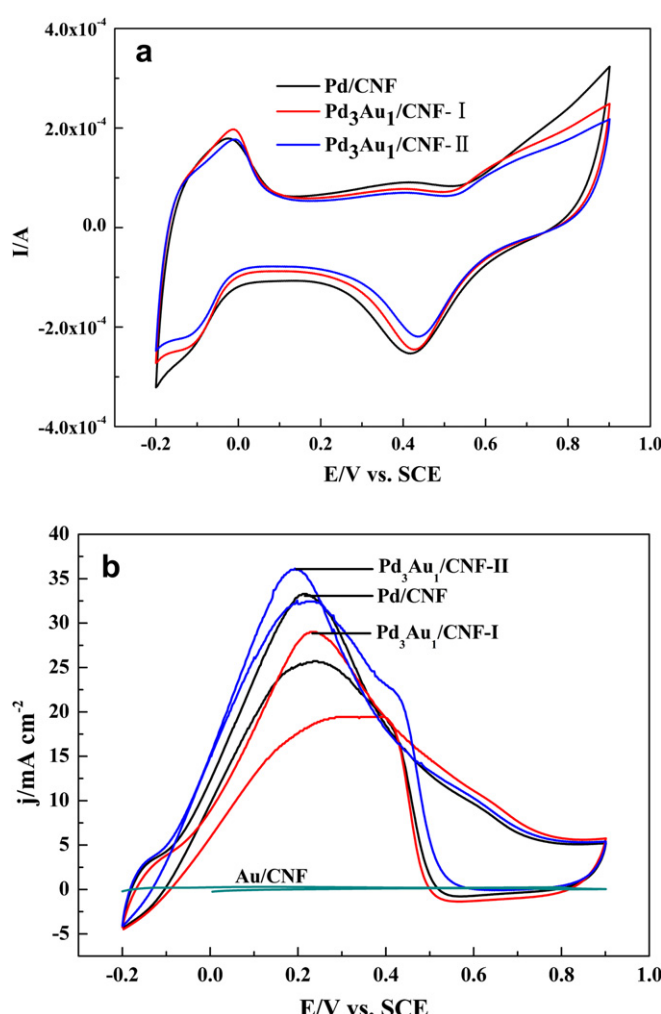
The mean particle size of PdAu particles in the $\text{Pd}_3\text{Au}_1/\text{CNF-II}$ catalyst is close to that of Pd particles in the highly dispersed and active Pd/C catalyst synthesized by Cheng et al. [5], while the mass activity of the former for formic acid oxidation is much higher than that of the latter ($0.63 \text{ mA mgPd}^{-1}$ vs. $0.52 \text{ mA mgPd}^{-1}$ based on the peak current density and the noble metal loading of each catalyst electrode), which may result from the electronic effect of Au on Pd for formic acid oxidation, namely by releasing the active sites on Pd surface for further electrocatalytic reaction.

Table 2

The values of peak potential, current density and mass activity of Pd/CNF, $\text{Pd}_3\text{Au}_1/\text{CNF-I}$ and $\text{Pd}_3\text{Au}_1/\text{CNF-II}$ catalysts for formic acid oxidation.

Samples	E_p/V	$j_p/\text{mA cm}^{-2}$	$j_m/\text{mA mgPd}^{-1}$
Pd/CNF	0.211	33.4	0.58
$\text{Pd}_3\text{Au}_1/\text{CNF-I}$	0.230	29.2	0.68
$\text{Pd}_3\text{Au}_1/\text{CNF-II}$	0.193	36.3	0.85

Fig. 3. Cyclic voltammograms of Au/CNF, Pd/CNF, $\text{Pd}_3\text{Au}_1/\text{CNF-I}$ and $\text{Pd}_3\text{Au}_1/\text{CNF-II}$ catalyst electrodes in 0.5 M $\text{H}_2\text{SO}_4 + 0.5$ M HCOOH solution with scanning rate of 50 mV s⁻¹ (the noble metal loading in each of the electrode was 4 μg).



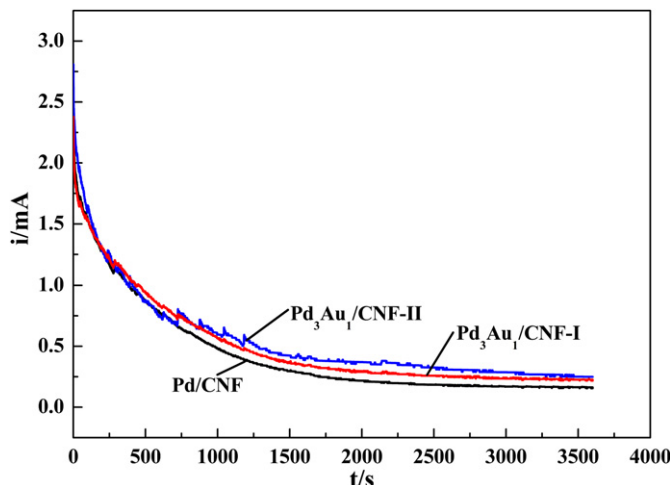


Fig. 4. Chronoamperometric curves of Pd/CNF, Pd₃Au₁/CNF-I and Pd₃Au₁/CNF-II catalyst electrodes in 0.5 M HCOOH + 0.5 M H₂SO₄ solution at the potential of 0.1 V (vs. SCE).

The electrocatalytic stability test for Pd/CNF, Pd₃Au₁/CNF-I and Pd₃Au₁/CNF-II catalysts for formic acid oxidation have been carried out by the chronoamperometry technique at a potential of 0.1 V (vs. SCE) in deaerated 0.5 HCOOH+0.5 M H₂SO₄ solution and the corresponding results are shown in Fig. 4. An initial decrease in the current density with time due to the intermediate poisoning species formed by formic acid oxidation can be observed at all catalysts. As expected, Pd₃Au₁/CNF-I and Pd₃Au₁/CNF-II catalysts demonstrate better electrocatalytic stability for formic acid oxidation than Pd/CNF catalyst due to the above mentioned electronic effect. Values of the current measured after 3600 s are 0.163, 0.226 and 0.249 mA on Pd/CNF, Pd₃Au₁/CNF-I and Pd₃Au₁/CNF-II catalysts, respectively, indicating that the addition of Au could improve the electrocatalytic stability of Pd for formic acid oxidation and the high-alloying Pd₃Au₁/CNF-II catalyst has a better electrocatalytic stability for formic acid oxidation than the low-alloying Pd₃Au₁/CNF-I catalyst.

4. Conclusions

In summary, PdAu nanoparticles with high- and low-alloying degrees were successfully supported on CNF supports. The

electrochemical measurements show that the addition of Au can promote the electrocatalytic activity of Pd/C catalyst for formic acid oxidation. The CNF supported high-alloying PdAu catalyst exhibits superior catalytic activity and stability over CNF supported low-alloying PdAu catalyst and the CNF supported Pd alone catalyst, which can be ascribed to the electronic effect of Au on Pd.

Acknowledgments

The present study was supported by the Nature Science Foundation of China (21073061), the open foundation of the State Key Laboratory of Electroanalytical Chemistry (Changchun Institute of Applied Chemistry, Chinese Academy of Sciences), Shanghai Key Laboratory of Green Chemistry and Chemical Process (East China Normal University) and the State Key Laboratory Breeding Base of Green Chemistry Synthesis Technology (Zhejiang University of Technology).

References

- [1] J. Wang, Y. Chen, H. Liu, R. Li, X. Sun, *Electrochim. Commun.* 12 (2010) 219–222.
- [2] S. Wang, N. Kristian, S. Jiang, X. Wang, *Electrochim. Commun.* 10 (2008) 961–964.
- [3] D. Morales-Acosta, J. Ledesma-Garcia, L.A. Godinez, H.G. Rodríguez, L. Álvarez-Contreras, L.G. Arriaga, *J. Power Sources* 195 (2010) 461–465.
- [4] H. Li, G. Sun, Q. Jiang, M. Zhu, S. Sun, Q. Xin, *Electrochim. Commun.* 9 (2007) 1410–1415.
- [5] N. Cheng, H. Lv, W. Wang, S. Mu, M. Pan, F. Marken, *J. Power Sources* 195 (2010) 7246–7249.
- [6] R. Larsen, S. Ha, J. Zakzeski, R.I. Masel, *J. Power Sources* 157 (2006) 78–84.
- [7] R. Wang, S. Liao, S. Ji, *J. Power Sources* 180 (2008) 205–208.
- [8] R. Larsen, J. Zakzeski, R. Masel, *Electrochim. Solid-State Lett.* 8 (2005) 291–293.
- [9] Y. Suo, I.M. Hsing, *Electrochim. Acta* 56 (2011) 2174–2183.
- [10] W. Zhou, J.Y. Lee, *Electrochim. Commun.* 9 (2007) 1725–1729.
- [11] J. Turkevich, P. Stevenson, J. Hillier, *Discuss. Faraday Soc.* 11 (1951) 55–75.
- [12] J. Turkevich, G. Kim, *Science* 169 (1970) 873–879.
- [13] G. Frens, *Nature* 241 (1973) 20–22.
- [14] J. Wilcockson, B. Abrams, *Chem. Soc. Rev.* 35 (2006) 1162–1194.
- [15] W. Zhou, J.Y. Lee, *J. Phys. Chem. C* 112 (2008) 3789–3793.
- [16] Y. Chen, Y. Tang, C. Liu, W. Xing, T. Lu, *J. Power Sources* 161 (2006) 470–473.
- [17] X. Wang, Y. Tang, T. Lu, *Electrochim. Acta* 14 (2008) 6–8.
- [18] J.-H. Zhou, Z.-J. Sui, P. Li, D. Chen, Y.-C. Dai, W.-K. Yuan, *Carbon* 44 (2006) 3255–3262.
- [19] Y. Xing, *J. Phys. Chem. B* 108 (2004) 19255–19259.
- [20] Y.-H. Qin, H.-C. Li, H.-H. Yang, X.-S. Zhang, X.-G. Zhou, L. Niu, W.-K. Yuan, *J. Power Sources* 196 (2011) 159–163.
- [21] E. Antolini, F. Cardellini, *J. Alloys Compd.* 315 (2001) 118–122.
- [22] X. Wang, Y. Tang, Y. Gao, T. Lu, *J. Power Sources* 175 (2008) 784–788.
- [23] B. Hammer, J. Nørskov, *Surf. Sci.* 343 (1995) 211–220.
- [24] J. Greeley, J.K. Nørskov, *Surf. Sci.* 592 (2005) 104–111.